

ESSENTIALS OF
**MODERN
OPEN-HOLE LOG
INTERPRETATION**

JOHN T. DEWAN

PennWell Books
PennWell Publishing Company
Tulsa, Oklahoma

generally a problem in empty holes, which are usually air drilled. However, hole rugosity may be a problem since extremely low-density material (air) is interposed between the pad and the formation. Much less rugosity can be tolerated in air-filled holes than in liquid-filled holes.

POROSITY DERIVATION FROM THE DENSITY LOG

Porosity is derived from bulk density in a very straightforward manner. For a clean formation with matrix (or grain) density ρ_{ma} , fluid density ρ_f , and porosity ϕ , the bulk density, ρ_b , is given by the summation of fluid and matrix components

$$\rho_b = \phi \cdot \rho_f + (1 - \phi) \rho_m \quad (5.2)$$

from which porosity is given by

$$\phi = (\rho_{ma} - \rho_b) / (\rho_{ma} - \rho_f) \quad (5.3)$$

Matrix densities in g/cc typically are

- $\rho_{ma} = 2.65$ for sands, sandstones, and quartzites
- $= 2.68$ for limey sands or sandy limes
- $= 2.71$ for limestones
- $= 2.87$ for dolomites

In liquid-bearing formations fluid density is typically that of the mud filtrate

- $\rho_f = 1.0$ for fresh mud
- $= 1.0 + 0.73 N$ for salt mud

where N is the sodium chloride concentration in $\text{ppm} \times 10^{-6}$.

Porosity may be derived from Fig. 5-5, which provides a graphical solution to Eq. 5.3. Bulk density is entered on the bottom scale and porosity is read on the vertical scale for appropriate values of ρ_{ma} and ρ_f . As an example, consider the interval 1,899-1,905 ft in Fig. 5-3 where the log density averages 2.29 g/cc. Assuming the formation is limestone and the fluid density is 1.0 (fresh-mud filtrate), the derived porosity from Eq. 5.3 or Fig. 5-4 is 24.5%.

It is more important to know the precise matrix density at low porosity than at high porosity. For example, at $\rho_b = 2.6$ g/cc, derived porosities would be 3% for sand and 6% for limestone. These differ by a factor of 2 and could mean the difference between expecting commercial and noncommercial production since a cutoff is often set around 5%. On the other hand,

Time
in
281
x
d
of
at
top
e
ing
for
in
in
in
ity of
ity of
and
enh
red o
g from
a ho
en

oks

Company

Heavy minerals in the formation such as pyrite (FeS_2) increase the effective matrix density and cause derived porosity to be too low if not taken into account. Occurrence is not frequent but is important in a few areas, particularly Alaska and the North Sea.⁴

Effect Of Gas

As described in chapter 1, considerable gas can be left in the flushed zone of a gas-bearing formation, bypassed by the invading filtrate. The density of the pore fluid can then be considerably less than one. Consequently, in gas-bearing formations there is a dual dilemma if the Density log is the only porosity curve run. First is recognizing that there is gas present, since the curve simply shows a decrease in bulk density that would normally be interpreted as an increase in fluid-filled porosity. Second is determining the correct porosity. It is not a straightforward matter. To apply Eq. 5.3, the fluid density, ρ_f , in the zone of investigation must be known. This depends on the water saturation in the invaded zone, S_{xo} , the mud filtrate density, ρ_{mf} , and the density, ρ_h , of the gas in the pores. That is

$$\rho_f = \rho_{mf} \cdot S_{xo} + \rho_h (1 - S_{xo}) \quad (5.4)$$

Gas density can be estimated from Fig. 5-6. However, S_{xo} is not known beforehand. If an R_{xo} curve is available, then

$$S_{xo} = c \sqrt{R_{mf}/R_{xo}} / \phi \quad (5.5)$$

If an R_{xo} curve is not available (usually the case with fresh mud), one can make an assumption such as

$$S_{xo} = S_w^{1/2} = [c \sqrt{R_w/R_t} / \phi]^{1/2} \quad (5.6)$$

Eqs. 5.3, 5.4, and 5.5 or 5.6 can be solved simultaneously or iteratively to give an apparent porosity ϕ_a . Allowing for the electron density effect gives a final porosity

$$\phi = \phi_a(0.93 + 0.07\rho_f) \quad (5.7)$$

As an example, consider the same interval (1,899-1,905 ft) in Fig. 5-3. Assume it is known to contain gas and that the electric logs give $R_w = 0.05$ and $R_t = 40$ ohm-m for this interval. From Fig. 5-6, $\rho_h = 0.07$ g/cc. Following the procedure outlined, using Eq. 5.6 $\phi = 17.5\%$. This porosity value differs significantly from the 24.5% found on the assumption of 100% liquid saturation.

This procedure is cumbersome and inaccurate, and it is rarely used. The Density log really needs outside help to establish matrix type, identify gas,

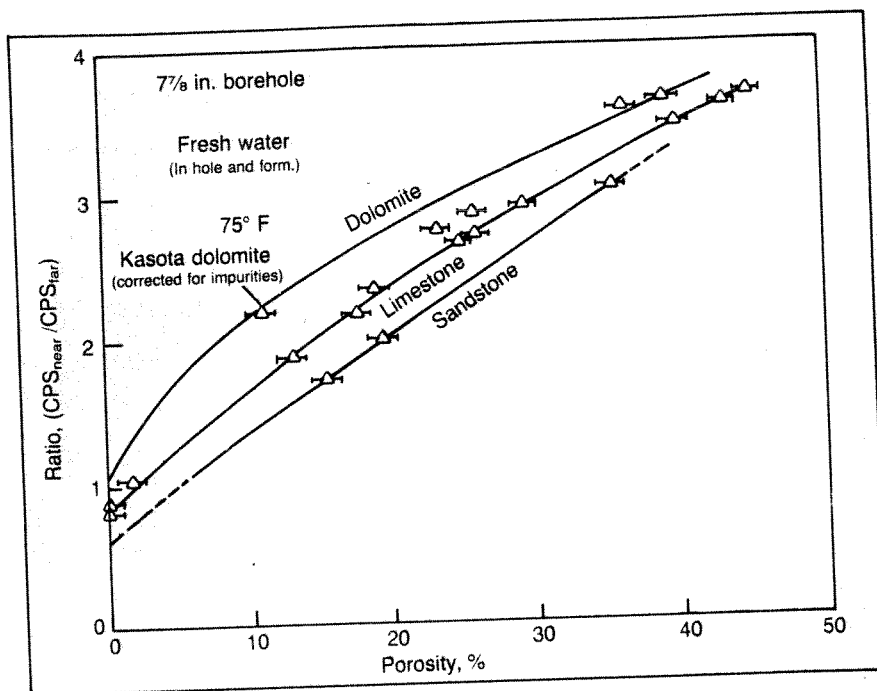


Fig. 5-14 CNL response in sandstone, limestone, and dolomite formations (courtesy Schlumberger, © SPE-AIME)

While the ratio depends primarily on porosity, there is also a significant dependence on lithology because the matrix contributes some to the slow-down and capture of the neutrons. It is clear that to derive porosity from the ratio with any accuracy, the lithology must be known.

Porosity Equivalence

Examination of Fig. 5-14 leads to a useful concept, that of equivalent porosities. Equivalent porosities are obtained by reading the dolomite, limestone, and sandstone porosities corresponding to a given ratio. For example, at a ratio of 2.0 we read 8% porosity for dolomite, 15% for limestone, and 19.5% for sandstone. These are equivalent porosities. Loosely speaking, neutrons slowing down and thermalizing cannot tell whether they are in one or the other of these equivalent formations.

Plotting porosity equivalents obtained at different ratios as a function of the limestone porosity corresponding to a given ratio leads to the porosity-

equivalence chart (porosities are read equivalent to a dolomite (lines A).

Porosity equivalent Fig. 5-15 (solid line) is partially to the lithology. In particular, the porosity of dolomites are sometimes present.

When a Comp. Rather, the ratio is

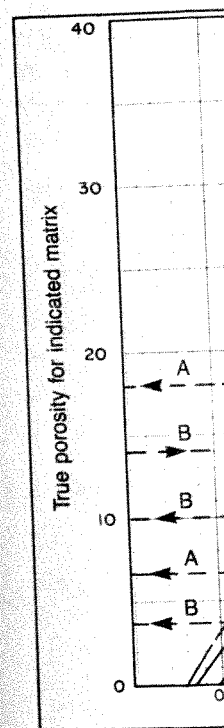


Fig. 5-15 Neut

equivalence chart of Fig. 5-15 (dashed lines) for the CNL. Equivalent porosities are read vertically. For example a limestone porosity of 14% is equivalent to a dolomite porosity of 7% or a sandstone porosity of 18% (lines A).

Porosity equivalents for the Sidewall Neutron (SNP) are also shown on Fig. 5-15 (solid lines). Matrix effects are less than for the CNL because epithermal detection eliminates neutron absorption effects that contribute partially to the lithology differences. Because of this, some operators still prefer the Sidewall Neutron over the Compensated Neutron at low porosities. In particular there is some uncertainty in the CNL response to very low-porosity dolomites apparently because of thermal neutron absorbers that are sometimes present in these formations in trace quantities.^{12,13}

When a Compensated Neutron log is run, the ratio is not recorded. Rather, the ratio is transformed to porosity, on the basis of laboratory data

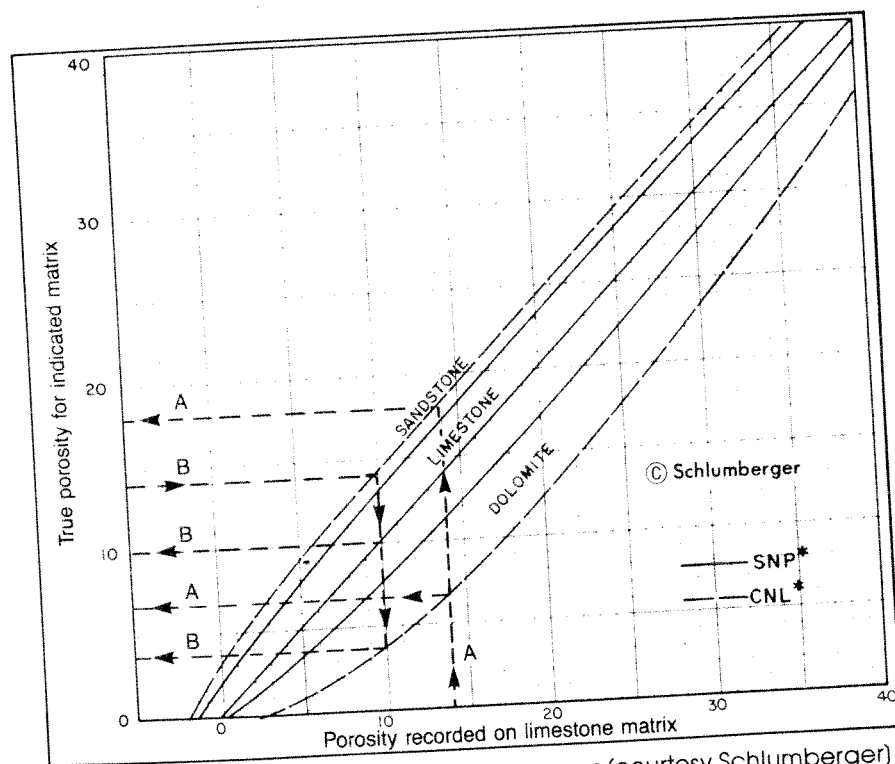


Fig. 5-15 Neutron porosity equivalence curves (courtesy Schlumberger)

such as that of Fig. 5-14, in a surface computer and a porosity curve is recorded. To effect the transformation, the logging engineer must input to the computer which matrix to use. He has a choice of limestone (LS) or sandstone (SS). The value chosen is the one most appropriate for the area and is shown on the log heading. It is left constant over the whole log even though the matrix may vary in intervals.

Depth of Investigation and Vertical Resolution

Fig. 5-16 shows the depth of investigation of the Compensated Neutron (CNL) tool in open hole at 22% porosity. For comparison those of the Sidewall Neutron (SNP) and Compensated Density (FDC) tools are also shown. None of the tools penetrates very deeply; but of the three the CNL has the greatest depth of investigation. It obtains 90% of its response from the first 10 in. of formation compared to 7 in. for the SNP and 4 in. for the FDC. Just as significant in terms of suppressing mud cake and rugosity effects is that the CNL receives only about 3% of its response from the first inch of formation compared to about 6% for the SNP and 17% for the FDC.

For the Neutron tools, depths of investigation will decrease slightly at higher porosities and increase somewhat at lower porosities. The reverse is true for the Density tool.¹⁴

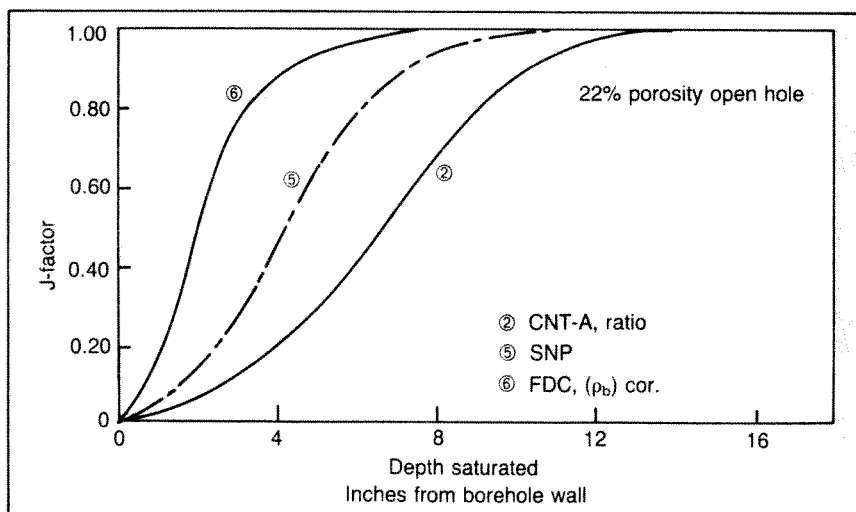


Fig. 5-16 Depth of investigation of Neutron and Density tools (courtesy Schlumberger, © SPE-AIME)

Vertical resolution of 15 in. However, with this speed, it is approximately the same porosity unit at very low porosity (the Density behavior). (The tool averages over about 3 ft)

Log Presentation

The Compensated Neutron tool is used to correct for matrix and clay effects. The Compensated Density and Gamma Ray tool is positioned adjacent to the Neutron tool so that the Density tool can be used to correct for the Neutron tool's response.

Fig. 5-18 shows the log presentation of the aforementioned combination. The log is recorded in Track 1, a Gamma Ray log in Tracks 2 and 3 with the Neutron tool. The Eastern Hemisphere tool is then transformed to porosity on the assumption of a limestone matrix.

Consider how the log is presented. The Gamma Ray shows a concern. Also the hole is not perfect. The errors are minimal.

The interval from 1 to 2 ft is limestone matrix. The interval from 2 to 3 ft is dolomite, porosity is 14%. A of Fig. 5-15. (Note that the log would be read as 14% if the matrix is limestone as indicated by lines B and C. The log is correct unless lithology is known.)

The same uncertainty in the interval Density porosity is shown in Fig. 5-5 and assuming the matrix is dolomite density, 2.68 g/cc, is given.

By combining Neutron and Density logs, lithology can largely be determined and the effect of

increased hydrogen fraction by weight.) As a result the Neutron curve, calibrated for liquid-filled porosity, indicates abnormally low porosity. The effect can be large. As an example, consider the zone from 1,884 ft to 1,922 ft of Fig. 5-20. This is a gas-bearing interval of porosity close to 18%, but the Neutron reads an average of about 5% porosity. This implies, as a first approximation, about $\frac{2}{3}$ of the pore space in the invaded zone is filled with gas (assumed at low pressure) and $\frac{1}{3}$ is filled with liquid. In reality, there is somewhat more liquid and less gas than that.

If the Neutron is the only porosity log run in potentially gas-bearing zones, there is the same dual dilemma as with the Density. First is to recognize the presence of gas, since it will appear on the log simply as lower porosity; if there are other low-porosity zones, as in Fig. 5-20, the gas will not stand out. Second is to derive the correct porosity because the gas saturation is not known beforehand.

The situation is further complicated because the *excavation effect* must be taken into account.¹⁶ This may be defined as the difference, in porosity units, between the Neutron log reading in a gas-bearing formation and that in a completely liquid-saturated formation having the same hydrogen content. The former will read lower porosity because it will contain less rock matrix, which will allow the neutrons to travel a little further. For example, a 30%-porosity formation with 50% water and 50% air in the pores would not read a porosity of 15%, as might be expected, but a porosity of 9%. The excavation effect would be 6 pu, which is not negligible. This difference is caused by the air space not being replaced by rock matrix.

An iterative procedure can be followed to obtain porosity in suspected gas-bearing zones. It is similar to that described for the Density log, utilizing electric logs to provide values of S_{xo} (Eqs. 5.5 or 5.6) and applying the excavation correction at every iteration. However, this procedure is exceedingly cumbersome and, as with lithology determination, can be replaced with simultaneous Density-Neutron interpretation.

COMBINED DENSITY-NEUTRON INTERPRETATION

Vastly improved and simplified log analysis is achieved when Density and Neutron interpretation are combined. Fig. 5-21 shows the crossplot chart obtained when Density response is plotted against Neutron porosity. It embodies the information in both Figs. 5-5 and 5-15.

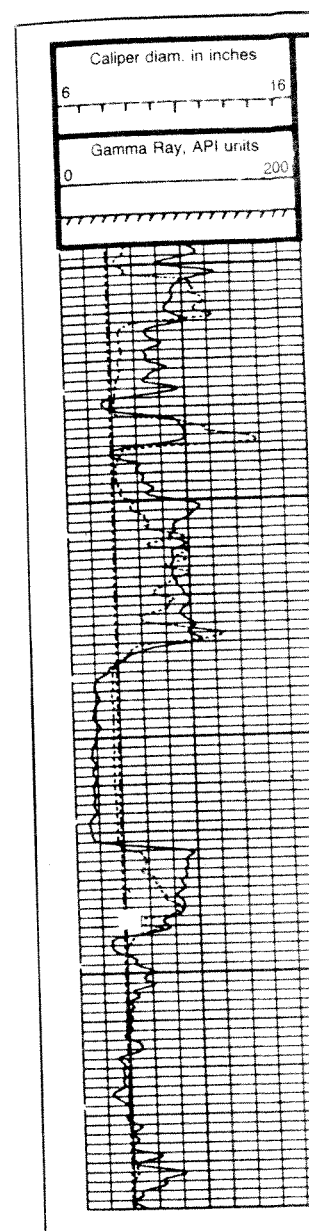


Fig. 5-20 Neutron-Density (Schlumberger)

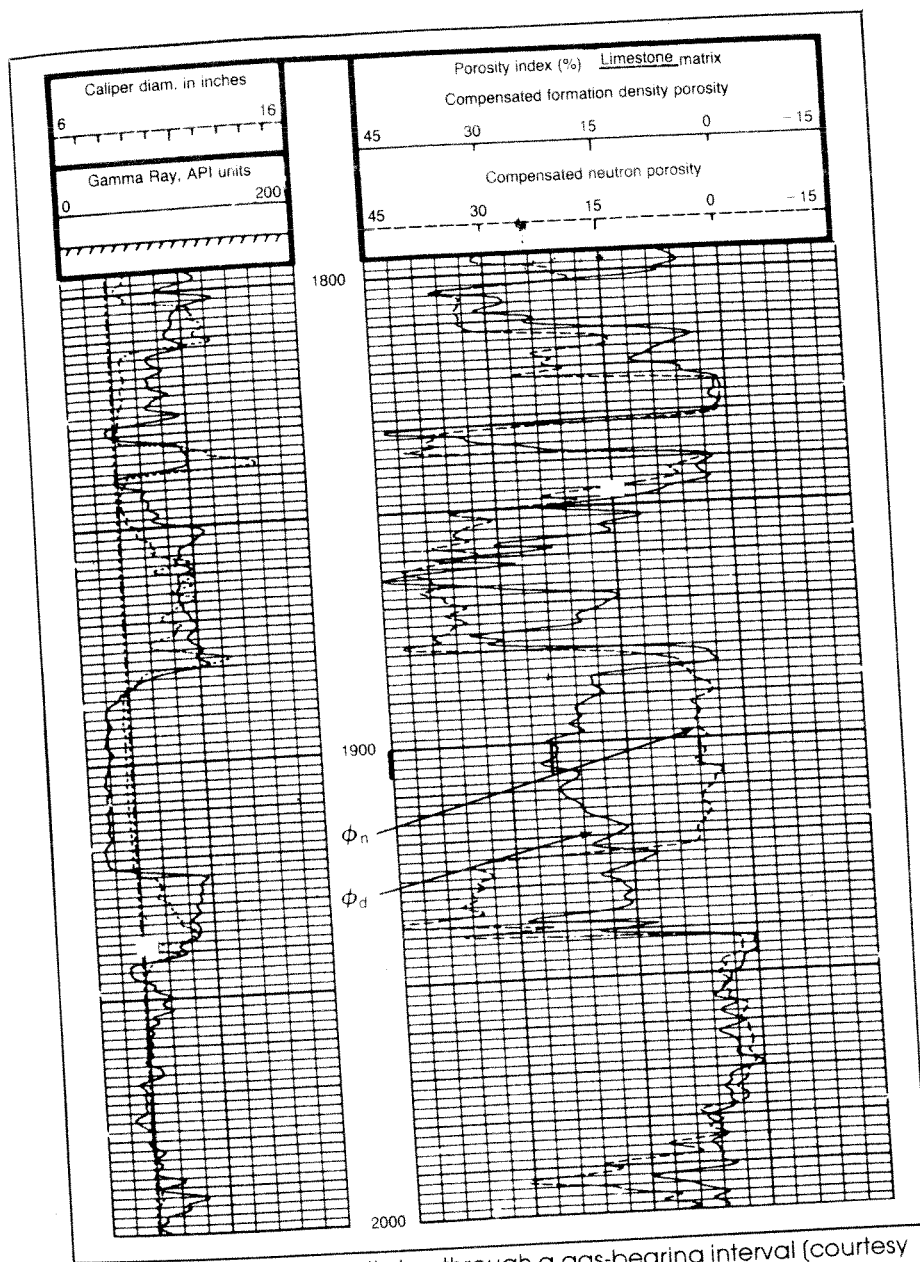


Fig. 5-20 Neutron-Density log through a gas-bearing interval (courtesy Schlumberger)

indicated as mostly dolomite with some limestone (probable) or some sandstone (less probable) or perhaps some of both; however, it could not be a mixture of limestone and sandstone.

Note that the bottom and right-hand scales of Fig. 5-21 can only be used if the log has been recorded on a limestone matrix. Had the same log been recorded on a sandstone scale, the intersection of $\phi_n = 14\%$ and $\phi_d = 2\%$ would be found by starting at those porosities on the sandstone line and projecting vertically and horizontally, respectively, to the point of intersection B. Porosity would still be determined as 8%, but lithology would be deduced as much less dolomite and more limestone or sandstone. To avoid confusion it is good practice to disregard the bottom and right-hand scales of the chart and use only the porosities on the limestone or sandstone curves (whichever the log heading indicates) as starting points. // *

Liquid-Filled Formations

All liquid-filled porosity points of usual lithology will fall inside the region bounded by the sandstone and dolomite lines. For this region a good approximation to the true porosity is the average of the Density and Neutron values

$$\phi = (\phi_d + \phi_n)/2 \quad \text{Liquid-Filled} \quad *$$

This is a most important result. Effective porosities can be eyeballed from the log as those values halfway between Density and Neutron curves for clean, liquid-filled formations. (If the Density porosity goes negative, its value should be taken as zero for this purpose.)

Looking again at Fig. 5-18 and using Fig. 5-21, we can deduce that the interval from 15,250 to 15,300 ft is primarily anhydrite of zero porosity and that at 15,381 to 15,385 ft, where the two curves agree, is limestone of 1.5% porosity. The log illustrates very nicely anhydrite, dolomite, and limestone signatures seen in tight carbonates.

Gas-Bearing Formations

As previously explained, replacement of liquid by gas in the pore space of rock causes both bulk density and hydrogen content to decrease. The Density will show higher porosity and the Neutron lower. This gives rise to the well-known crossover effect on Neutron-Density logs. Normally, the Neutron reads somewhat higher porosity than Density due to dolomitization and to clay effects. When the Neutron crosses over and reads lower porosity than the Density, it is an infallible indicator of gas (except for one qualification given below). This is a very popular feature of the Density-Neutron combination.

Fig. 5-20 is an excellent example. Throughout the interval shown, the Neutron reads equal to (within statistics) or higher than the Density except in the 1,884 to 1,922 ft zone where there is a marked crossover. This interval is clearly gas bearing. The question is, what is the correct porosity?

Referring to the crossplot chart (Fig. 5-21), gas will cause intersection points to shift northwesterly and in many cases will cause them to fall above the sandstone line. For the interval 1,900 to 1,905 ft of Fig. 5-20 where $\phi_n = 6$ and $\phi_d = 24.5\%$, the point of intersection is at C. To find the porosity, the point is shifted back to the assumed lithology line (in this case limestone) in a direction parallel to the gas correction line indicated. In this case the porosity is found as 17.5% (point D).

A good approximation to the true porosity in gas-bearing zones is

$$\phi = \sqrt{(\phi_d^2 + \phi_n^2)/2} \quad (5.13)$$

In the case illustrated this formula gives $\phi = 18\%$, which agrees with the value obtained graphically. This leads to the eyeball rule that in gas-bearing zones the porosity is not midway between Neutron and Density values but is about $\frac{2}{3}$ of the way from the Neutron to the Density reading.

The gas correction line indicated applies to the situation where both Density and Neutron are responding to the same condition, that is, when depth of invasion exceeds 12 in. (from the borehole wall) or is practically nil. Even in this case the slope of the line depends a little on the porosity and on the density and composition of the gas, which is the reason the line is labeled "approximate."

In situations where the depth of invasion is in the range 4-6 in., the Density will respond only to the invaded zone, whereas the Neutron will "see" well into the noninvaded zone. In gas-bearing intervals the invaded zone will have lower gas saturation than the noninvaded region, perhaps by a factor of two. The appropriate gas correction line then becomes significantly closer to horizontal. Use of the indicated line results in underestimating porosities. In the extreme situation of 4-6 in. of invasion and practically no gas in the invaded zone, the correction line is virtually horizontal.

Precise correction requires running an R_{xo} log and combining derived S_{xo} , d_i , and S_w values with applicable depth of investigation data for the Density and Neutron. This normally is not done but could lead to improved interpretation in gas-bearing zones.

False Gas Indication

There is one circumstance where a false indication of gas can be obtained from Neutron-Density crossover. This is the situation where the porosity

curves are recorded on limestone. Referring to Fig. 5-22 limestone matrix—will show Density porosity of 13% (1) simply a matrix effect.

Fig. 5-22 is an example of primarily sandstone, but the whole interval appears gas sandstone matrix, 3.5 pu sl subtracted from the Density (a few thin beds that appear vals much of the residu enlargement (short cave) el

The clue to false gas inc difference between the Ne effect should be suspected.

By the same token, gas c on sandstone matrix and trated. The gas shift might not cause the Neutron to cr see with a dolomite matrix. dolomite causes the Neutro Fig. 5-18), which can supp as this, it is important to h

The Litho-Density log c Fig. 5-23 is an example fi Neutron combination was and dolomites. Scales are s overlay (approximately) in crossovers occur, and in ot could be interpreted as gas

The P_e curve, however crossovers are limestones (F over are dolomites ($P_e = 3$) dolomites to be gas-bearing tion of a few tight streaks prime use of the Litho-De gas and matrix effects in ti

1.8–2.2 in accordance with $m = 1.8 + 0.6 \text{ CEC}_{\text{sh}}$, since increased clay surface area implies increased tortuosity. Conductivities so calculated are compared to measured shale conductivities in Fig. 7–9.

The agreement between calculated and measured values is remarkable, considering that the comparison covers 16 wells from Louisiana to California with depths ranging from 2,000–15,000 ft, CEC_{sh} values ranging from 0.02–0.7, and temperatures ranging from 100–275°F. Some of the spread between measured and calculated values can certainly be attributed to logging tool averaging. CEC_{sh} values for cores taken within 1–2 ft of each other varied by a factor of 1.4, which corresponds to factor-of-two variations in calculated conductivities.

The D-W model therefore explains why shale porosities can vary all the way from 2% to 35% and resistivities can vary from 0.3 to 100 ohm-m. This being the case, it should work well for shaly sands. * *

APPLICATION OF THE DUAL-WATER METHOD TO SHALY SANDS

For practical application we shall use the following form of the D-W saturation relation, derived from Eq. 7.13 by replacing conductivities by resistivities ($C = 1/R$) and rearranging terms

$$S_{\text{wt}}^2 - S_{\text{wt}} \cdot S_b(1 - R_w/R_b) = R_w/(R_t \cdot \phi_t^2) \quad (7.23)$$

The second term of this relation applies the shale correction. If it is omitted, the expression reverts to the familiar Archie relation. To apply the equation, the parameters S_b , ϕ_t , R_w , and R_b must be determined. First consider S_b , the bound water fraction in the shaly sand. *
*
*

From Eqs. 7.5 and 7.18, S_b may be written as the following ratio (also called normalized Q^{18})

$$S_b = Q/Q_{\text{sh}} \approx 0.3 Q \quad (7.24)$$

To determine S_b accurately requires a direct measurement of Q ; a Q -log is sorely needed. Unfortunately, no such log is currently available, although measurements on cores can be readily made in the laboratory or even at the wellsite.^{19,20} Consequently, we are forced into indirect methods using shale indicators.

In terms of V_{sh} , the volumetric fraction of shale (including its bound water), the effectively porosity, ϕ_e , can be written

$$\phi_e = \phi_t - V_{\text{sh}} \cdot \phi_{\text{tsh}} \quad (7.25)$$

where ϕ_t is the total porosity of the shaly sand and ϕ_{tsh} is the total porosity of the shale fraction in the sand. Equating this expression to that of Eq. 9.6 gives

$$S_b = V_{sh} \cdot \phi_{tsh} / \phi_t \quad (7.26)$$

Determination of S_b therefore reduces to obtaining V_{sh} from available shale indicators. This is a key result.

Evaluation of V_{sh}

No single logging measurement accurately measures V_{sh} . Consequently, V_{sh} is usually estimated from several shale indicators and the lowest value is used.^{21,22} The two best indicators are the Density-Neutron difference and the GR log. A fallback indicator that is less reliable is the SP log. All techniques assume that the shale in a shaly sand is the same as that in adjacent shales. This is a reasonable premise for sands with shale laminations, but it is very questionable for sand with dispersed clay. Nevertheless, there is no alternative.

1. V_{sh} from the Density-Neutron Difference

Because of the lattice-bound hydrogen in clay, a gas-free shaly sand will always read a higher Neutron porosity than Density porosity, as illustrated by the differences in Tables 7-2 and 7-3. The larger the fraction of shale, the greater the difference. The effect is linear, so the shale fraction is given by

$$(V_{sh})_{ND} = (\phi_n - \phi_d) / (\phi_{nsh} - \phi_{dsh}) \quad (7.27)$$

where the numerator represents the difference in Neutron and Density porosities in the shaly sand and the denominator represents the difference in nearby shale. The latter will typically be 0.15 to 0.30, depending on the amount and type of clay in the shale.

This method cannot be used when gas is present or suspected since gas distorts the ϕ_n and ϕ_d values.

2. V_{sh} from The Gamma Ray Log

Gamma Ray deflection increases with shale content of a formation. Consequently, an index of the degree of shaliness of a sand is obtained by linearly interpolating between the clean sand level and the shale level

$$I_{sh} = (GR - GR_{cl}) / (GR_{sh} - GR_{cl}) \quad (7.28)$$

where

GR = reading in

GR_{cl} = average re

GR_{sh} = average re

I_{sh} will vary from zero i

Estimation of the cl
7-10 is not always easy
vary considerably in a
occasional abnormally

The fractional volur
the density of the form
situation when thin sha
of the same bulk densit
7-11, converting I_{sh} to

On the other hand
substantial increase in
the pores of originally c
7-11 transforming I_{sh} to
extremes. Consequently
applied when a Density

where ρ is the density o
nearby shale. The expo
mined precisely.

Where spectral Gan
in certain areas by elin
using only the Th + K c
prominent, the potassi
One field study report
values measured on cor
CEC values.²⁵ This w
montmorillonate and
respectively, along with
hand the Neutron-Dens
chlorite, which have lo
Gamma Ray as the bet

Best
method

except
when
gas
present

*

Can't
have gas

*

GR

where

- GR = reading in the sand of interest, APIU
 GR_{cl} = average reading in nearby clean sands, APIU
 GR_{sh} = average reading in nearby 100% shales, APIU

I_{sh} will vary from zero in a clean sand to 1.0 in shale.

Estimation of the clean sand and 100% shale levels, as illustrated in Fig. 7-10 is not always easy. There may be few clean sands and the shales may vary considerably in activity, so a good deal of judgment is required. An occasional abnormally high shale reading should be ignored.

The fractional volume of shale, V_{sh} , will be equal to the shale index, I_{sh} , if the density of the formation does not vary with shale content. This is the situation when thin shale laminations are intermixed with clean sand layers of the same bulk density. In this case the straight-line relationship of Fig. 7-11, converting I_{sh} to V_{sh} , applies.

On the other hand when increasing clay content is accompanied by a substantial increase in bulk density, as it is when authigenic clay grows in the pores of originally clean high-porosity sands, then the curved line of Fig. 7-11 transforming I_{sh} to V_{sh} applies.²³ Many cases will fall between the two extremes. Consequently, a more generally applicable relation that might be applied when a Density log accompanies the Gamma Ray is

$$(V_{sh}) = I_{sh} \cdot (\rho/\rho_{sh})^3 \quad (7.29)$$

where ρ is the density of the formation of interest and ρ_{sh} is the density of nearby shale. The exponent 3 is an educated guess; it has never been determined precisely.

Where spectral Gamma Ray logs are run, improvement may be effected in certain areas by eliminating the U component and determining $(V_{sh})_{GR}$ using only the Th + K components. If feldspars or micaceous formations are prominent, the potassium component should be eliminated or subdued.²⁴ One field study reported excellent correlation between $(V_{sh})_{GR}$ and CEC values measured on cores and poor correlation between $(V_{sh})_{ND}$ and the same CEC values.²⁵ This was attributed to the GR responding primarily to montmorillonate and illite, with high uranium and potassium contents respectively, along with these clays having high CEC values. On the other hand the Neutron-Density separation gives greatest weight to kaolinite and chlorite, which have low CEC values. This is an argument in favor of the Gamma Ray as the better CEC indicator.

t of linko,
oleum
in 1981,
er for
s and
reading
develop-
ed no
ding
payers
efforts in

gno n
reedy of
ceedy of
n
h and
n
cantly
eered in
n from
n, h
e 1980

oks
iny

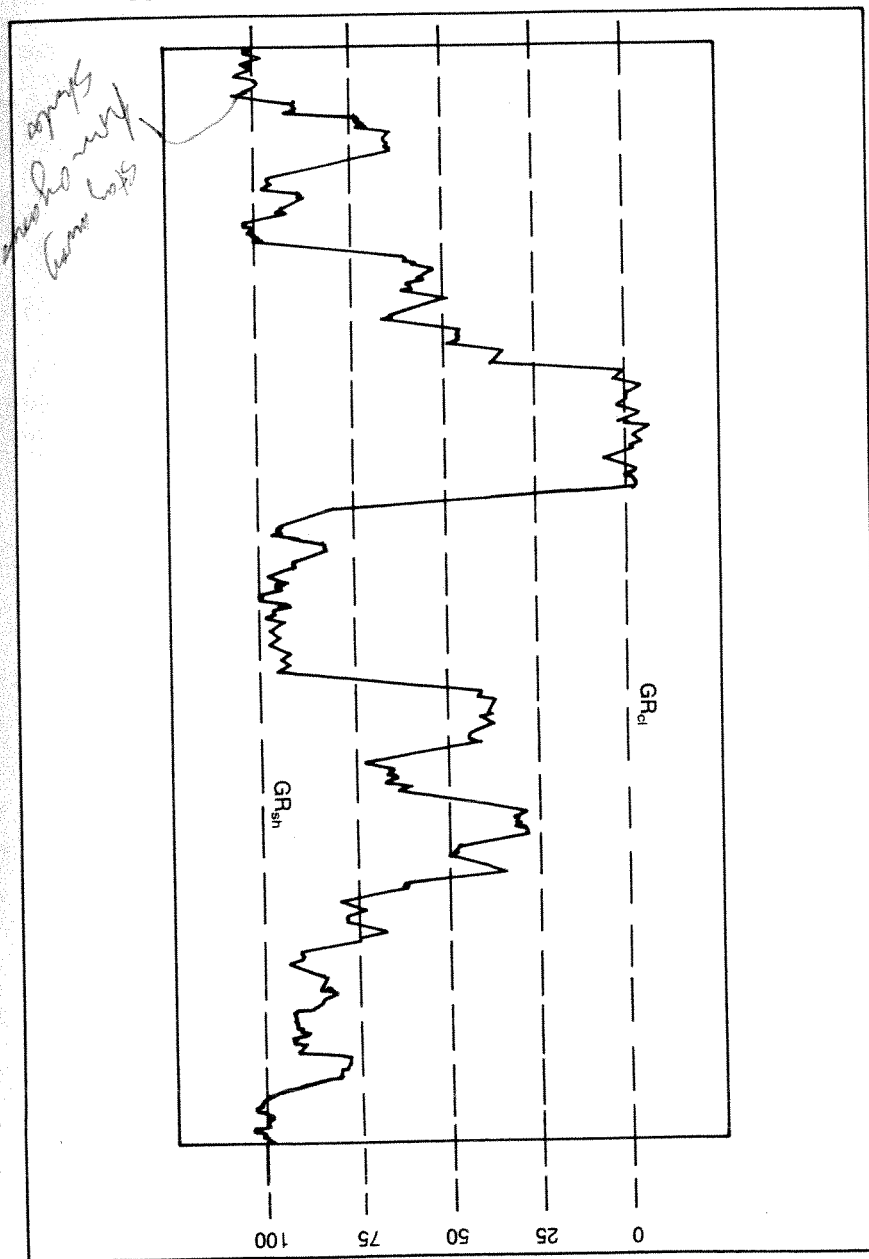


Fig. 7-10 Determination of shale indication, I_{sh} , from the GR curve

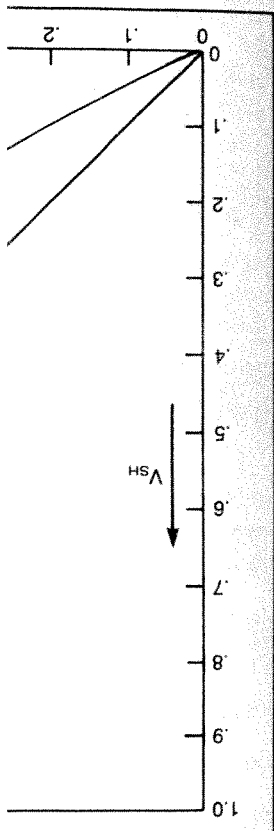


Fig. 7-11 Conversion of V_{sh} from the SP L (courtesy Schlumber)

3. V_{sh} from the SP L. In similar fashion, V_{sh} where the numerator is the zone of interest and the difference between the only under certain conditions. With several V_{sh} values as the lowest value as the correlation indicated. The reason is

3. V_{sh} from the SP Log

In similar fashion, V_{sh} can be calculated from the SP log as

$$(V_{sh})_{SP} = (SP - SP_{cl}) / (SP_{sh} - SP_{cl}) \quad (7.30)$$

where the numerator is the difference in millivolts between the SP level in the zone of interest and the clean formation level and the denominator is the difference between the shale and clean levels (the SSP). This relation is valid only under certain conditions, as pointed out in Chapter 3.

With several V_{sh} values so determined, standard procedure is to pick the lowest value as the correct one, excluding the crossplot value when gas is indicated. The reason is that most side effects cause calculated V_{sh} values to

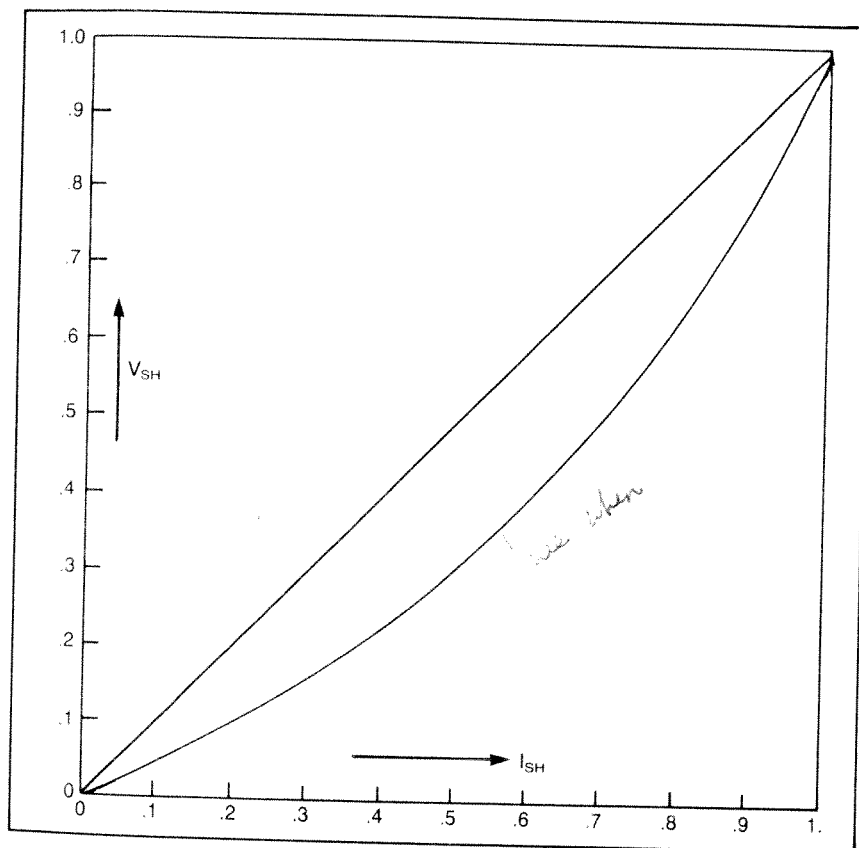


Fig. 7-11 Conversion of GR shale indication, I_{sh} , to shale fraction, V_{sh} (courtesy Schlumberger, © SPE-AIME)

Timko,
m.
1981,
or
and
ng
elop-
ne
gging
ger's
arts in
ee in
sity of
ety of
and
tents
pred a
g from
y, he
ben-

oks
any

be too high. Heavy minerals or neutron absorbers in the shaly sand will cause $(V_{sh})_{ND}$ to be too large. Hole enlargements in the shales will cause $(V_{sh})_{GR}$ to be too great; it is particularly important to correct the GR readings when caving is severe and the mud weight is high before computing V_{sh} . Hydrocarbons in the shaly sand will often cause $(V_{sh})_{SP}$ to be too high. Consequently, the lowest value is picked, but even it is not likely to be very accurate.

Determination of Effective Porosity

The next step is to determine the effective porosity, ϕ_e , of the shaly sand. The Density and Neutron porosities are first corrected for shale as follows

$$\phi_{dc} = \phi_d - V_{sh} \cdot \phi_{dsh} \quad (7.31)$$

$$\phi_{nc} = \phi_n - V_{sh} \cdot \phi_{nsh} \quad (7.32)$$

If no gas is present, the corrected porosities should be close together. The effective porosity can be taken as the average

$$\Rightarrow \phi_e = (\phi_{dc} + \phi_{nc})/2 \quad (7.33)$$

If gas is present, it will show up as a crossover or enhanced crossover of the corrected porosities, ϕ_{nc} being significantly less than ϕ_{dc} . This is the main reason for proceeding in this fashion. With gas the effective porosity may be taken as

$$\Rightarrow \phi_e = \sqrt{(\phi_{dc}^2 + \phi_{nc}^2)/2} \quad (7.34)$$

The effect of these calculations is illustrated in the crossplot of Fig. 7-12, which applies to sand or limestone provided the porosity values input correspond to the matrix chosen. On such a plot, clean formation points fall along the 45° line and shaly formation points fall to the right of the line. Gas-bearing formations will plot to the left if not too shaly. The shale point, S, may fall anywhere in the indicated shale zone, depending on the type and content of clay in the shale. Point P represents a gas-free shaly formation point. Correcting for shale translates this point to P_1 (parallel to the line OS), and averaging porosities at P_1 gives the effective porosity, P_2 .

If the same sand contained gas, it would show up as some point such as P_3 on the plot. Correcting for shale moves that point to P_4 , accentuating the gas effect. Correcting for gas via Eq. 7.34 is equivalent to translating point P_4 to the 45° line in a direction parallel to the gas correction line. This brings P_4 back essentially to P_2 .

Determination of
Unfortunately, there i
clay densities may var
ity (based on 2.65 g/cc
low.) The Neutron po
equation is

where δ is a constant b
The total porosity,
sand are then

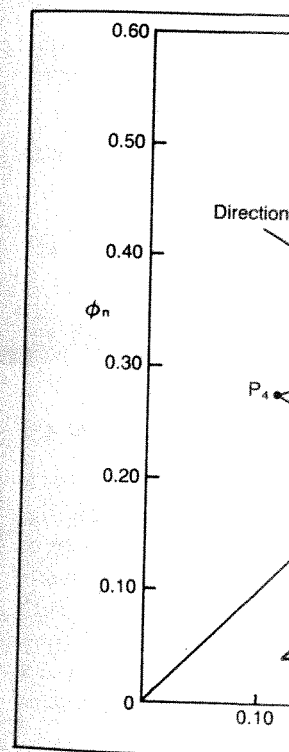


Fig. 7-12 Co

Determination of ϕ_{tsh} , the total porosity of the shale, is required next. Unfortunately, there is no accurate method of measuring this quantity. Dry clay densities may vary all the way from 2.4–3.0 g/cc, so the Density porosity (based on 2.65 g/cc) may be too high or too low; (most often it will be too low.) The Neutron porosity will always be too high. Therefore, a common equation is

$$\phi_{tsh} = \delta \phi_{dsh} + (1 - \delta) \phi_{nsh} \quad (7.35)$$

where δ is a constant between 0.5 and 1.0, depending on local experience.

The total porosity, ϕ_t , and the bound-water fraction, S_b , for the shaly sand are then

$$\phi_t = \phi_e + V_{sh} \cdot \phi_{tsh} \quad (7.36)$$

$$S_b = V_{sh} \cdot \phi_{tsh} / \phi_t \quad (7.37)$$

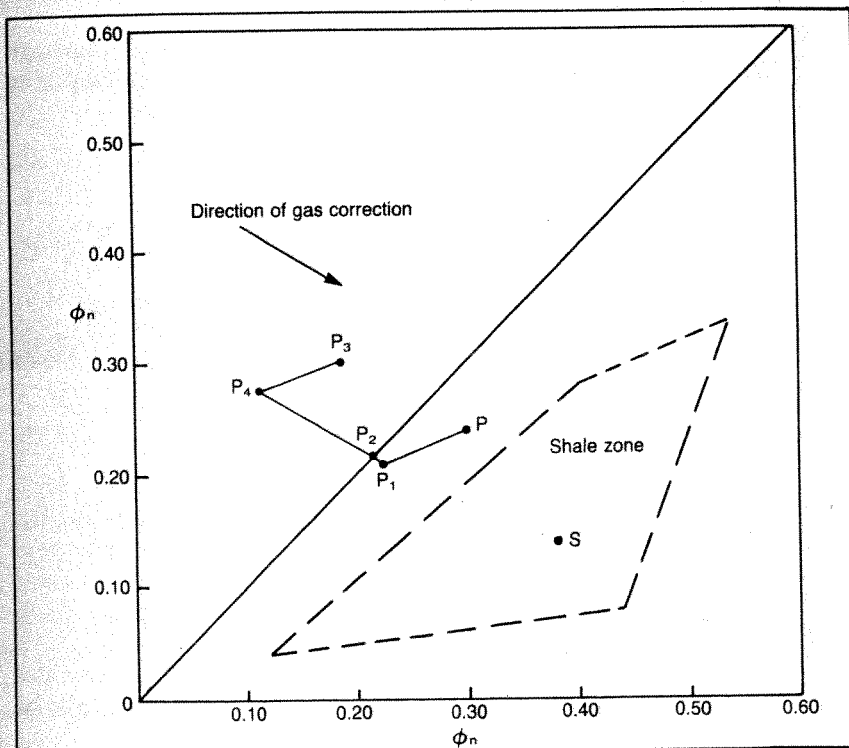


Fig. 7-12 Correction for shale and gas effects

Basic Well Log Analysis

(Second Edition)

By
George Asquith and Daniel Krygowski
(with sections by Steven Henderson and Neil Hurley)

AAPG Methods in Exploration Series 16

Published by
The American Association of Petroleum Geologists
Tulsa, Oklahoma

Figure 1.11. Chart for adjusting fluid resistivities for temperature.
(Schlumberger, 1998, Figure Gen-9.)

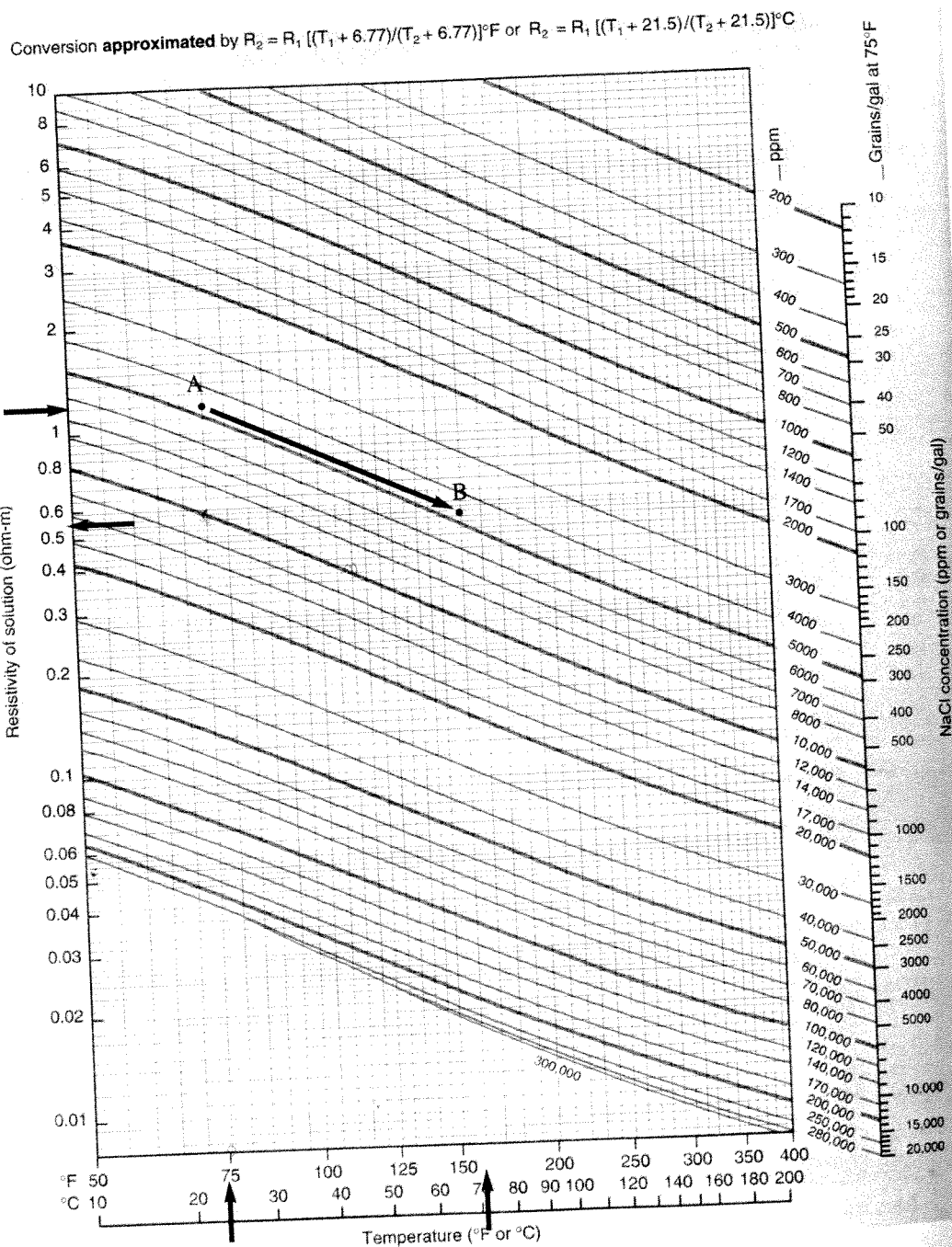
Given:

Resistivity of drilling mud (R_m) equals 1.2 ohm-m at 75°F.
Formation temperature (T_f) = 160°F.

Procedure:

1. Locate the resistivity value, 1.2 ohm-m, on the scale at the left of the chart.
2. Move to the right horizontally along the 1.2 ohm-m line until the vertical line representing a temperature of 75°F (from the bottom of the chart) is encountered (point A on the chart).
3. Move parallel to the (diagonal) constant salinity line to where it intersects the vertical line representing a temperature value of 160°F (point B on the chart).
4. From point B, follow the horizontal line to the left to determine the resistivity of the fluid at the desired temperature (0.58 ohm-m at 160°F).

Each diagonal line on the chart shows the resistivity of a solution of fixed concentration over a range of temperatures. The diagonal lines at the bottom of the chart indicate that an NaCl solution can hold no more than 250,000 to 300,000 ppm NaCl depending on temperature (i.e., the solution is completely salt saturated).



Estimating Geohydrologic Properties from Borehole-Geophysical Logs

by Donald G. Jorgensen

Abstract

Borehole-geophysical logs can be used to estimate geohydrologic properties based on in situ measurement of rock and water properties. Estimates of properties of both formation and water, such as coefficient of diffusion, formation factor, cementation exponent, hydraulic conductivity, irreducible water content and specific yield can be assessed from borehole-geophysical data and selected algorithms and graphs.

Water properties, such as resistivity, sodium chloride concentration, viscosity and density, can also be estimated using data from borehole-geophysical logs. Water resistivity using the spontaneous-potential method can be estimated if an empirical correction for fresh water is applied.

Estimates of formation properties, such as porosity and permeability, can also be made using borehole-geophysical data.

Introduction

Borehole-geophysical logs corrected for borehole environmental effects can be used to estimate geohydrologic properties needed to evaluate the ground water resource including, but not limited to, properties that relate to the quantity of water and water chemistry. Selected lithologic properties that affect the occurrence, movement, and chemistry of water can also be deduced from borehole-geophysical logs. Geohydrologic properties that can be estimated from these logs include water resistivity, sodium chloride concentration, dissolved-solids concentration, viscosity, bulk density, formation factor, cementation exponent, hydraulic conductivity, irreducible water content, specific yield, and coefficient of diffusion.

This paper draws freely from an earlier publication by the author (Jorgensen 1989) and in some respects is an addendum to that paper. However, this paper describes some new and little-known techniques of determining geohydrologic properties.

The purpose of this paper is to show, mainly by example, methods for estimating geohydrologic or lithologic properties (or to reference publications that describe such procedures).

Background Relations

Conductivity and Resistivity

In the saturated zone, the most frequently run borehole-geophysical logs are variations of resistivity logs or conductivity logs (conductivity is the reciprocal of resistivity). One model of conductivity assumes that

total conductivity is the sum of the conductivity of the water in the effective (interconnected) porosity, the conductivity of the bound water along grains, the conductivity due to ion exchange, and the conductivity of the matrix (formation material).

Because conductivity is the reciprocal of resistivity, the total resistivity in ohms is as follows:

$$\frac{1}{r_t} = \frac{1}{r_{ep}} + \frac{1}{r_{bw}} + \frac{1}{r_{ie}} + \frac{1}{r_{mat}} \quad (1)$$

where

r_t is the total resistivity

r_{ep} is the resistivity due to water in the effective porosity, either primary or secondary

r_{bw} is the resistivity of bound water (water bound to the walls of the effective pores)

r_{ie} is the resistivity related to ion exchange

r_{mat} is the resistivity of the rock matrix, exclusive of effective porosity.

Formation Factor and Resistivity of Water

The usual practice in petroleum investigations is to assume the last three terms of Equation 1 are negligible, so that

$$\frac{1}{r_t} = \frac{1}{r_{ep}} \quad (2)$$

However, this assumption is not completely true for aquifer material containing fresh water because the

Porosity can be determined from a neutron, sonic, nuclear-magnetic-resonance log or under certain conditions from analysis of other logs.

Examples of Estimating Geohydrologic Properties

Permeability

An example of log interpretation to estimate permeability is taken from logs of a test hole in Kansas (Jorgensen 1989). Figure 2 is based on a log-log cross plot of the resistivity value, R_o , determined from a deep-looking induction log, and the porosity, (ϕ) , determined from neutron and gamma-gamma logs.

Based only on the information shown for point 5 on Figure 2, which is assumed typical; the average porosity is 0.13, R_w is 0.38 ohm m at 82 F, and m is 1.37. Using Equation 12, permeability (k) is calculated as follows:

$$k = 84,000 \frac{(0.13)^{1.37+2}}{(1.0-0.13)^2} = 115 \text{ millidarcies} = 1.14 \times 10^{-13} \text{ m}^2 \quad (15a)$$

Sodium Chloride Concentration of Water

Relations between water resistivity and sodium chloride concentration are well established and discussed in published literature, such as Jorgensen (1989). Keys (1988) modified information of Alger (1966) and presented a graphical representation of the relation among resistivities, temperatures, and concentrations (Figure 3). An example of estimating sodium chloride concentration (C_{NaCl}) follows:

An R_w of 0.38 ohm m at 82 F was determined by the cross-plot method for formation water for the test hole in Kansas (Figure 2). The value exceeds 10,000 milligrams per liter (mg/L) and, thus, is beyond the range of sodium chloride concentration curves shown in Figure 3. However, C_{NaCl} can be estimated easily without resorting to graphs.

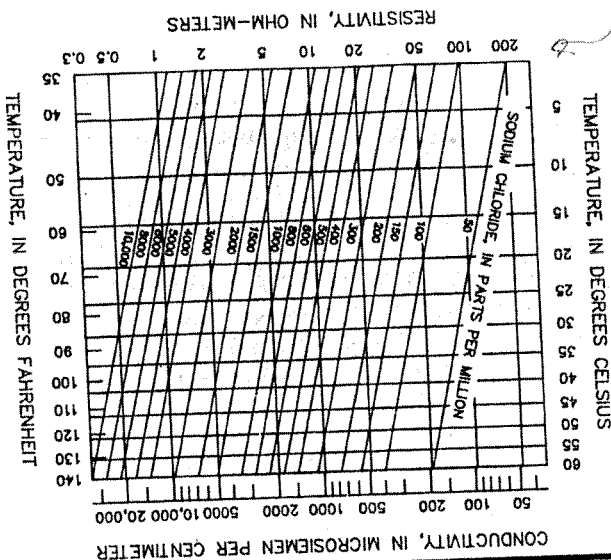


Figure 3. Relation among resistivities, temperatures, and concentrations for dilute sodium chloride solutions (modified from Alger 1966 and Keys 1988).

Intuitively, equations for estimating permeability that include irreducible-water content (S_{wi}) should be more accurate than Equation 12. An example is the Coates relation which follows:

$$k = 100 \frac{\phi^2 (1-S_{wi})}{S_{wi}} \quad (13)$$

where S_{wi} is dimensionless irreducible water content expressed as a decimal and is equivalent to specific retention.

S_{wi} is not easily determined from the usual borehole geophysical logs. However, the response of a nuclear-magnetic-resonance (NMR) log is reported to be a function of S_{wi} . Unfortunately, these logs are relatively new, and the equipment to conduct them is not always readily available. However, if S_{wi} could be determined from an NMR log, application of Equation 13 (Coates and Dumanior 1973) should be relatively easy. Schlumberger Educational Services (1987) gives the following equation:

$$RFI = \phi(1-S_{wi}) \quad (14)$$

where RFI is the free fluid index as recorded on a nuclear-magnetic-resonance log (NML) and relates to fluid that is "free to move; that is not bound or trapped." Under certain conditions, permeability can also be related to responses recorded on an acoustic log. Specifically, attenuation of the Stoneley wave has been correlated to permeability (Taylor and others 1989). The technique uses information from a full-wave form acoustic log. The method is promising but the complete usefulness of the method is undetermined at present and discussion of the method is beyond the scope of this paper.

Specific Yield

If irreducible saturation is approximately equal to specific retention, then specific yield can be estimated by the following equation:

$$S_y = \phi - S_{wi}$$

Basic Well Log Analysis

(Second Edition)

By

George Asquith and Daniel Krygowski
(with sections by Steven Henderson and Neil Hurley)

AAPG Methods in Exploration Series 16

Published by

The American Association of Petroleum Geologists
Tulsa, Oklahoma

Gamma Ray

GENERAL

Gamma ray (GR) logs measure the natural radioactivity in formations and can be used for identifying lithologies and for correlating zones. Shale-free sandstones and carbonates have low concentrations of radioactive material and give low gamma ray readings. As shale content increases, the gamma ray log response increases because of the concentration of radioactive material in shale. However, clean sandstone (i.e., with low shale content) might also produce a high gamma ray response if the sandstone contains potassium feldspars, micas, glauconite, or uranium-rich waters.

In zones where the geologist is aware of the presence of potassium feldspars, micas, or glauconite, a spectral gamma ray log can be run in place of the standard the gamma ray log. The spectral gamma ray log records not only the number of gamma rays emitted by the formation but also the energy of each, and processes that information into curves representative of the amounts of thorium (Th), potassium (K), and uranium (U) present in the formation.

If a zone has a high potassium content coupled with a high gamma ray log response, the zone might not be shale. Instead, it could be a feldspathic, glauconitic, or micaceous sandstone.

Like the SP log, gamma ray logs can be used not only for correlation, but also for the determination of shale (clay) volumes. These volumes are essential in calculating water saturations in shale-bearing formations by some shaly-sand techniques. Unlike the SP log, the gamma ray response is not affected by formation water resistivity (R_w), and because the gamma ray log responds to the radioactive nature of the formation rather than the electrical nature, it can be used in cased holes and in open holes containing nonconducting drilling fluids (i.e., oil-based muds or air).

The gamma ray log is usually displayed in the left track (track 1) of a standard log display, commonly with a caliper curve. Tracks 2 and 3 usually contain

porosity or resistivity curves. Figure 3.1 is an example of such a display.

SHALE VOLUME CALCULATION

Because shale is usually more radioactive than sand or carbonate, gamma ray logs can be used to calculate volume of shale in porous reservoirs. The volume of shale expressed as a decimal fraction or percentage is called V_{shale} . This value can then be applied to the analysis of shaly sands (see Chapter 7).

Calculation of the gamma ray index is the first step needed to determine the volume of shale from a gamma ray log:

$$I_{GR} = \frac{GR_{log} - GR_{min}}{GR_{max} - GR_{min}} \quad 3.1$$

where:

I_{GR} = gamma ray index

GR_{log} = gamma ray reading of formation

GR_{min} = minimum gamma ray (clean sand or carbonate)

GR_{max} = maximum gamma ray (shale)

Unlike the SP log, which is used in a single linear relationship between its response and shale volume, the gamma ray log has several nonlinear empirical responses as well as a linear response. The nonlinear responses are based on geographic area or formation age, or if enough other information is available, chosen to fit local information. Compared to the linear response, all nonlinear relationships are more optimistic; that is, they produce a shale volume value lower than that from the linear equation. For a first-order estimation of shale volume, the linear response, where $V_{shale} = I_{GR}$, should be used.

The nonlinear responses, in increasing optimism (lower calculated shale volumes), are:

Larionov (1969) for Tertiary rocks:

$$V_{sh} = 0.083(2^{3.7 I_{GR}} - 1) \quad 3.2$$

Steiber (1970):

$$V_{sh} = \frac{I_{GR}}{3 - 2 \times I_{GR}} \quad 3.3$$

Clavier (1971):

$$V_{sh} = 1.7 - [3.38 - (I_{GR} - 0.7)^2]^{1/2} \quad 3.4$$

Larionov (1969) for older rocks:

$$V_{sh} = 0.33 \times (2^{2 I_{GR}} - 1) \quad 3.5$$

See Figures 3.1 and 3.2 for an example of a shale volume calculation using the gamma ray log.

SPECTRAL GAMMA RAY LOG

The response of the normal gamma ray log is made up of the combined radiation from uranium, thorium, potassium, and a number of associated daughter products of radioactive decay. Because these different radioactive elements emit gamma rays at different energy levels, the radiation contributed by each element can be analyzed separately. Potassium (potassium 40) has a single energy of 1.46 MeV (million electron volts). The thorium and uranium series emit radiation at various energies; however, they have prominent energies at 2.614 MeV (thorium) and 1.764 MeV (uranium). By using energy-selective sensor windows, the total gamma ray response can be separated into the gamma rays related to each of these elements (Dewan, 1983). Figure 3.3 illustrates one format used to display output from the spectral gamma ray log. In addition to the individual elements shown in tracks 2 and 3, the spectral gamma ray data can be displayed in track 1 as total gamma radiation (SGR-dashed curve) and total gamma radiation minus uranium (CGR-solid curve).

Important uses of the spectral gamma ray log include (Dresser-Atlas, 1981):

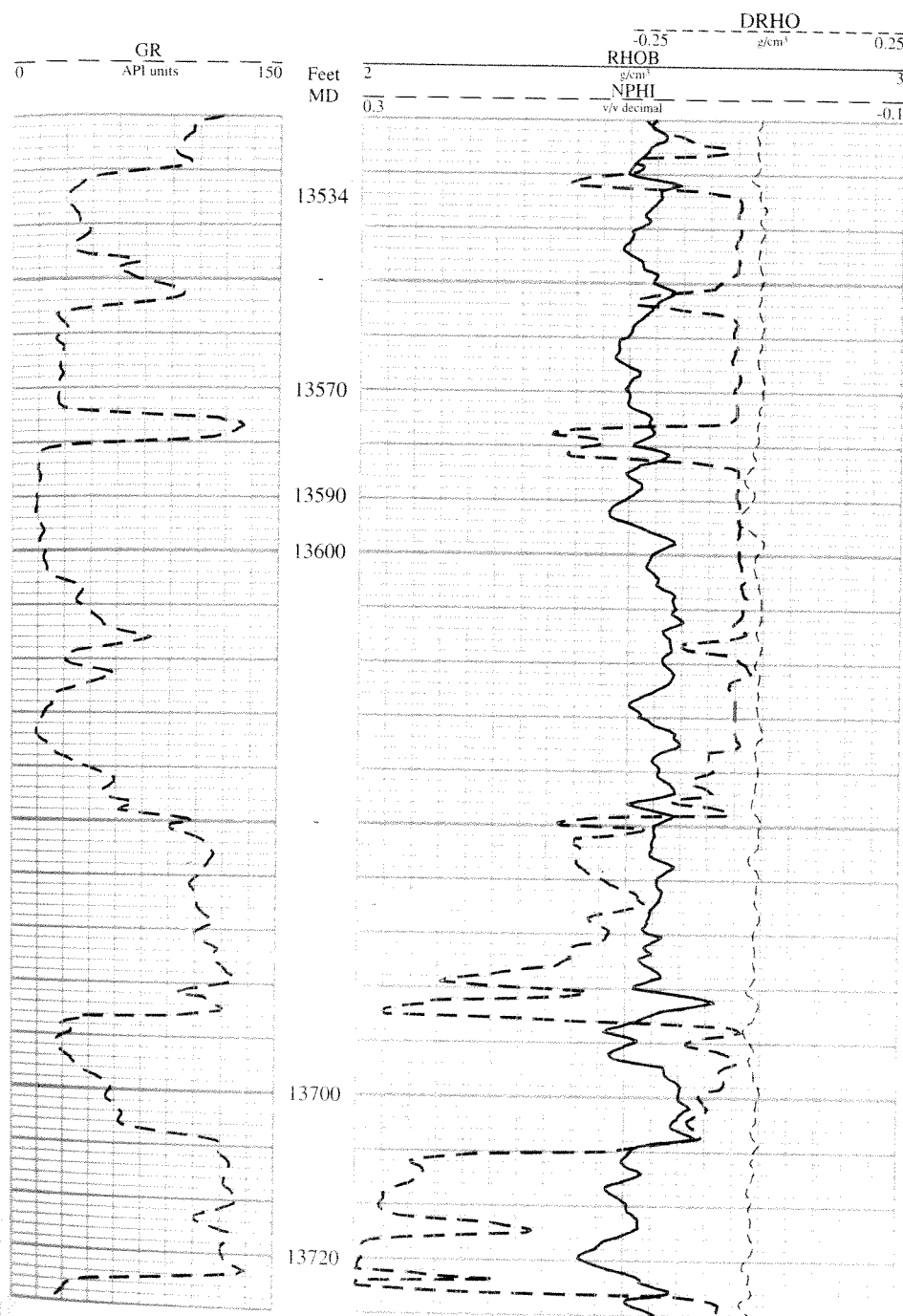
- determining shale (clay) volume (V_{shale}) in sandstone reservoirs that contain uranium minerals, potassium feldspars, micas, and/or glauconite
- differentiating radioactive reservoirs from shales
- source-rock evaluation
- evaluation of potash deposits
- geologic correlations
- clay typing
- fracture detection
- rock typing in crystalline basement rocks

In most log analyses, the first two uses listed above are the most important uses of spectral log data.

In determining shale volume (V_{shale}) in sandstones, Dewan (1983) has suggested the use of only the thorium and potassium components instead of total GR in the V_{shale} equations, because uranium salts are soluble and can be transported and precipitated in the formation after deposition. If potassium minerals are present in the sandstone, Dewan (1983) suggested the use of only the thorium component in the V_{shale} equations. Radioactive reservoirs like the "hot" dolomites of the Permian (west Texas and New Mexico) and Williston (Montana, North Dakota, and South Dakota) basins of the United States are normally differentiated from shales by the low thorium and potassium contents and high uranium content.

REVIEW

1. Gamma ray logs are lithology logs that measure the natural radioactivity of a formation.
2. Because radioactive material is concentrated in shale, shale has a high gamma ray reading. Shale-free sandstones and carbonates, therefore, usually have low gamma ray readings.
3. Gamma ray logs are used to identify lithologies, correlate between formations, and calculate volume of shale.



Depth (ft)	GR_{log}	I_{GR}
13,534	32	0.16
13,570	28	0.12
13,701	55	0.35

See Figure 3.2 to convert I_{GR} to shale volume (V_{shale}).

Figure 3.1. Example of a gamma ray log with neutron-density log.

This example illustrates the curves and scales of a gamma ray log, and is also used to pick values for Figure 3.2.

Track 1 (to the left of the depth track): The gamma ray log (GR) is the only one represented on this track. Note that the scale increases from left to right, and ranges from 0 to 150 API gamma ray units in increments of 15 API units.

Tracks 2 and 3 (used together, to the right of the depth track): These tracks include logs representing bulk density (RHOB), neutron porosity (NPHI), and density correction (DRHO). Bulk density (RHOB) is represented by a solid line and ranges from 2.0 to 3.0 g/cm³ increasing from left to right. Neutron porosity (NPHI) is represented by a dashed line and ranges from -0.10 (-10%) to +0.30 (30%) increasing from right to left. The correction curve (DRHO) is represented by a dotted line and ranges from -0.25 to +0.25 g/cm³ increasing from left to right, but only uses track 3.

Calculation of Gamma Ray Index I_{GR} for Shale Volume Calculation

The minimum gamma ray value (GR_{min}) occurs at 13,593 ft and is 14 API units (slightly less than 1 scale division from zero).

The maximum gamma ray value (GR_{max}) occurs at 13,577 ft and at 13,720 ft and is 130 API units. These are the shaliest zones in the interval.

The gamma ray readings from three depths are shown in the table below.

From Equation 3.1, the gamma ray index (I_{GR}) is:

$$I_{GR} = \frac{GR_{log} - GR_{min}}{GR_{max} - GR_{min}} \quad 3.6$$

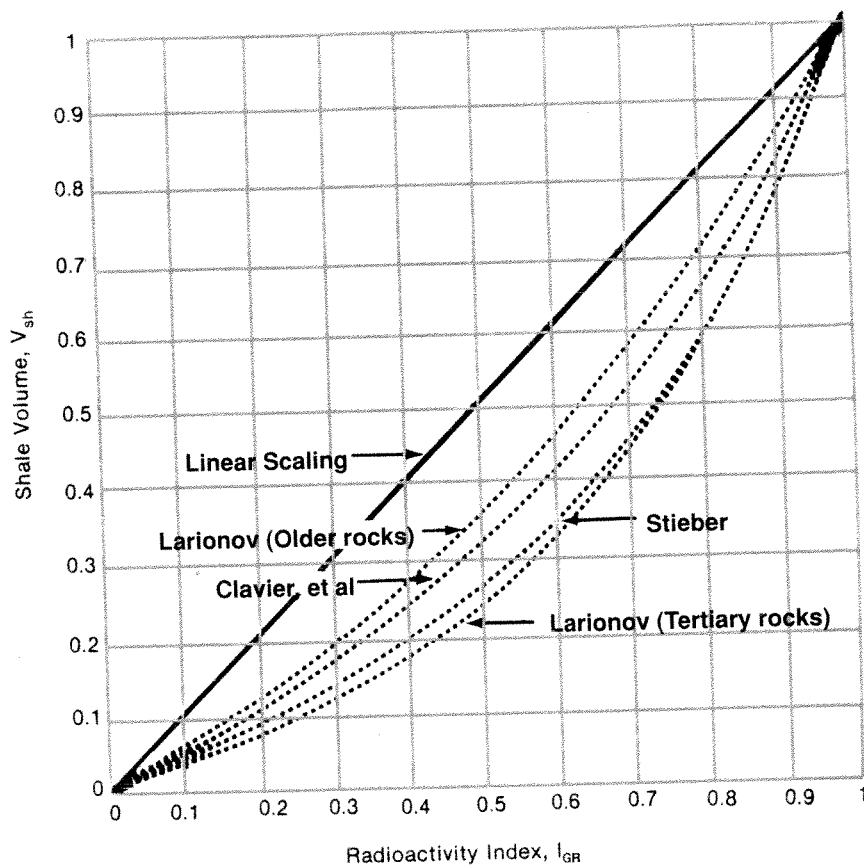
Figure 3.2. Chart for correcting the gamma ray index (I_{GR}) to the shale volume (V_{shale}). (Western Atlas, 1995, Figure 4-24)

Given (from Figure 3.1):

Depth (ft)	GR_{log}	I_{GR}
13,534	32	0.16
13,570	28	0.12
13,701	55	0.35

Procedure:

1. For each zone below, find the gamma ray index value (I_{GR}) on the horizontal scale on the bottom.
2. Follow the value vertically to where it intersects curve each of the curves listed below.
3. From each curve, move horizontally to the scale at the left and read the shale volume. This is the amount of shale in the formation expressed as a decimal fraction.



Courtesy Baker Atlas, ©1996-1999 Baker Hughes, Inc.

Depth (ft)	GR_{log}	I_{GR}	Shale volume, V_{shale}		
			Linear	Larionov (for rocks older than Tertiary)	Stieber
13,534	32	0.16	0.16	0.08	0.06
13,570	28	0.12	0.12	0.06	0.04
13,701	55	0.35	0.35	0.21	0.15

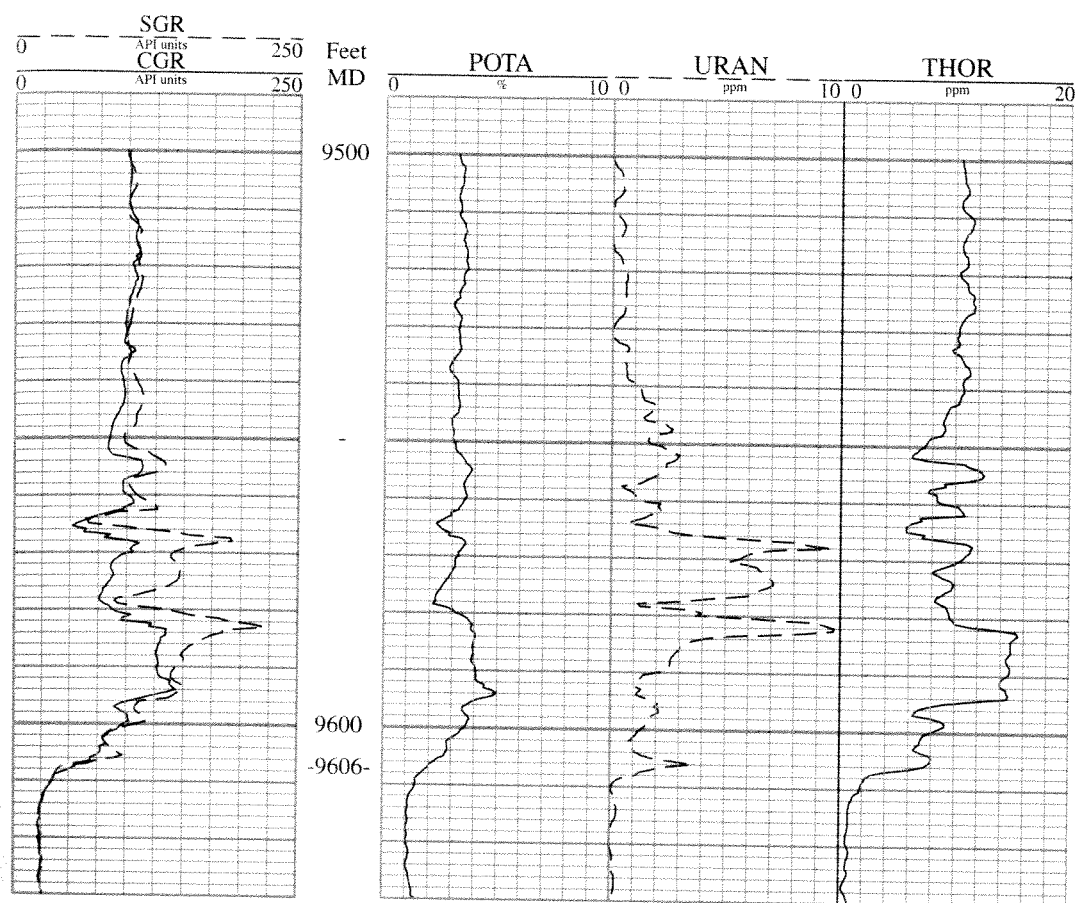


Figure 3.3. Spectral gamma ray log.

This example is from West Texas. The Mississippian Barnett Shale contacts the underlying Mississippian limestone at 9606 ft. In the Barnett Shale, note the great variations in the potassium (POTA), uranium (URAN), and thorium (THOR) contents above the contact with the Mississippian limestone indicating changes in shale mineralogy.

Symbols:

- SGR Total gamma ray (dashed curve, track 1)
- CGR Total gamma ray minus uranium (solid curve, track 1)
- POTA Potassium 40 in weight percent (tracks 2 and 3)
- URAN Uranium in ppm (tracks 2 and 3)
- THOR Thorium in ppm (tracks 2 and 3)

Table 4.2. Matrix densities and photoelectric-effect (P_e) values of common lithologies (Courtesy Halliburton, 1991).

Lithology/ Fluid	ρ_{ma} or ρ_{fl} g/cm ³ [Kg/m ³]	P_e (b/e)
Sandstone	2.644 [2644]	1.81
Limestone	2.710 [2710]	5.08
Dolomite	2.877 [2877]	3.14
Anhydrite	2.960 [2960]	5.05
Salt	2.040 [2040]	4.65
Fresh water	1.0 [1000]	
Salt water	1.15 [1150]	
Barite (mud additive)		267

Importance of Correct ρ_{ma} and ρ_{fl} values

A computer in the logging unit calculates density porosity from the measured bulk density of the formation using Equation 4.7. The wellsite geologist or logging unit engineer specifies the matrix and fluid densities that are to be used. If the formation's actual matrix density (ρ_{ma}) is less than the matrix density used to calculate the porosity [e.g., calculating porosity of a sandstone ($\rho_{ma} = 2.64$ g/cm³) using a limestone matrix density ($\rho_{ma} = 2.71$ g/cm³)], the log shows a calculated porosity that is higher than the actual porosity of the formation. If the formation's actual fluid density is less than the fluid density used to calculate the porosity [e.g., calculating the porosity of a saltwater-filled formation ($\rho_{fl} = 1.1$ g/cm³) using a freshwater value ($\rho_{fl} = 1.0$ g/cm³)], the log shows a calculated porosity that is lower than the actual porosity of the formation. Because of the wider range of matrix-density values than fluid-density values, errors in estimating the matrix density have a larger impact on the calculated porosity.

Bulk-density values from selected depths on the log in Figure 4.3 are listed in Table 4.7. Those values are used in the chart in Figure 4.4 to determine density porosity, which is listed in Table 4.8.

Hydrocarbon Effects

Where invasion of a formation is shallow, the low density of the formation's hydrocarbons causes the calculated density porosity to be greater than the actual porosity. Oil does not significantly affect density porosity, but gas does (gas effect). Hilchie (1978) suggests using a gas density of 0.7 g/cm³ for fluid density

ty (ρ_{fl}) in the density-porosity formula if gas density is unknown. Because the presence of oil has little effect on the density log, this tool usually provides the best indication of porosity in liquid-filled holes.

Heavy Minerals

Any time the bulk density of a formation (ρ_b) is greater than the assumed matrix density (ρ_{ma}) of the formation [e.g., when measurements are made in an anhydrite ($\rho_{ma} = 2.96$ g/cm³) but are recorded using a limestone matrix ($\rho_{ma} = 2.71$ g/cm³)], the resulting density porosity is negative. It is important to note that in cases like this the logging tool is operating properly, but the assumptions made in the conversion between bulk density and density porosity are incorrect. In cases like this, where the porosity is clearly erroneous (because it is negative), the log still yields good information. Negative density porosity is often a good indication of the presence of anhydrite or other heavy minerals, as shown in Figure 4.5 over the intervals 11,550 to 11,567 ft and 11,600 to 11,618 ft.

Powdered barite is commonly added to mud to increase mud density. When heavy muds are used (e.g., 14 lb/gal), the high P_e of the barite (Table 4.2) in the mud can mask the P_e of the adjacent rock layers.

NEUTRON LOG

Neutron logs are porosity logs that measure the hydrogen concentration in a formation. In clean formations (i.e., shale-free) where the porosity is filled with water or oil, the neutron log measures liquid-filled porosity (ϕ_N , PHIN, or NPHI).

Neutrons are created from a chemical source in the neutron logging tool. The chemical source is usually a mixture of americium and beryllium which continuously emit neutrons. When these neutrons collide with the nuclei of the formation the neutron loses some of its energy. With enough collisions, the neutron is absorbed by a nucleus and a gamma ray is emitted. Because the hydrogen atom is almost equal in mass to the neutron, maximum energy loss occurs when the neutron collides with a hydrogen atom. Therefore, the energy loss is dominated by the formation's hydrogen concentration. Because hydrogen in a porous formation is concentrated in the fluid-filled pores, energy loss can be related to the formation's porosity.

The neutron curves are commonly displayed over tracks 2 and 3, in units referenced to a specific lithology (usually either limestone or sandstone, depending on the geologic environment expected to be encountered), as illustrated in Figure 4.5.

1
50
0.3 - 1.0 g/cm³

Price \$6.50

U.S. DEPARTMENT OF COMMERCE
BUREAU OF ECONOMIC ANALYSIS

USE OF GEOPHYSICAL LOGS TO ESTIMATE WATER-QUALITY TRENDS IN CARBONATE AQUIFERS

By L. M. MacCary

ABSTRACT

This report describes the use of well-log analysis to determine the water-quality trends in carbonate aquifers by use of apparent water resistivities (R_{wa}). The data were obtained from geophysical logs run by the U.S. Geological Survey or purchased from Petroleum Information Corporation and from sample logs purchased from American Stratigraphic Company (Amstrat logs)¹. Drill-stem test data and water analyses of oil and water test wells in parts of Montana, North and South Dakota, and Wyoming were obtained from the computer files of the U.S. Geological Survey.

Depending on rock and mud resistivities, two useful resistivity curves for water-quality studies are the deeply-focused laterolog and the induction log. For older wells, the standard electric log may be the only resistivity curve available; it, too, can be used in some instances. The preferred porosity logs are the sonic, sidewall neutron, compensated neutron, and the density log. Wells drilled before the 1960's were generally logged with an uncalibrated neutron curve. In some instances, this curve can be empirically calibrated, but frequently the resulting porosities are anomalous compared to core porosities, or those determined from modern logs.

The wells described in this report penetrated both limestone and dolomite; the highest porosity zones are within the dolomitic rocks. Experience gained during the Madison Limestone project indicates that meaningful R_{wa} values cannot be calculated when rock porosities are less than 7 percent. Accuracy of R_{wa} calculations can be improved when water analyses are available from drill-stem tests or pumped samples. Ionic content of the water is recast as an equivalent sodium chloride solution and resistivity of this solution is determined graphically or calculated. Resulting resistivities are used to develop the parameter m in the R_{wa} equation.

R_{wa} contour maps derived from geophysical data are useful to outline areas of recharge, direction of probable ground-water flow and location and salinity of brine areas.

¹Use of brand names in this report is for identification and does not imply endorsement by the U.S. Geological Survey.